The 2009 IEEE/RSJ International Conference on
Intelligent Robots and Systems
October 11-15, 2009 St. Louis, USA

Experimental Study of A Parametrically Excited Dynamic Bipedal Walker with Counterweights

Takeshi Hayashi, Fumihiko Asano, Zhi-Wei Luo, Akinori Nagano, Kazuaki Kaneko and Atsuo Kato

Abstract— **This paper reports some interesting results on our experimental study of parametrically excited dynamic bipedal walking. We describe the details of the walking machine that has telescopic legs, semicircular feet, free hip-joint and counterweights. The walker can sustain stable dynamic walking on level ground based on mechanical energy restoration in accordance with the principle of parametric excitation utilizing the effects of semicircular feet and counterweights. Results of numerical analysis of the effect of the counterweights on the gait efficiency are also described.**

I. INTRODUCTION

Recently, many efficient dynamic bipedal walkers have been developed [1]. They are inspired by McGeer's research on passive dynamic walking (PDW) [2], and effectively utilize the principle dynamics.

Asano *et al*. on the other hand proposed a method for generating efficient dynamic bipedal gait based on the principle of parametric excitation [3]. In this method, a biped robot can restore the mechanical energy lost by heel strike by pumping the leg mass in accordance with parametric excitation, and achieve stable gait generation very easily. Here by using telescopic leg, both mechanical energy restoration and obstacle avoidance can be simultaneously realized. Although the legs are straight, the walker can avoid foot-scuffing during the stance phase by lifting the swing leg [4][5]. In addition, the robot has semicircular feet because this approach does not require ankle-joint actuation. Semicircular feet are very effective to realize efficient dynamic bipedal gait because their rolling effect provides virtual ankle-joint torque [6][7] and they reduce the mechanical energy dissipation caused by heel strike [8]. Based on the observations, we have developed a walking machine that has telescopic legs, semicircular feet, free hip-joint, and counterweights.

In our previous works [3], we reported the development of the walker, however, due to several problems, sustainable level dynamic walking had been achieved only up to 5 steps. In this paper we will propose a new bipedal walker model that has a counterweight on each leg. This paper then reports the final experimental walking machine with counterweights and its walking results. In detail, we observed more than 8 steps with the probability of one fourth in the experiment. It is also investigated through numerical simulations how the counterweights attached on the hip affects the gait stability and efficiency.

T. Hayashi, Z.W. Luo and A. Nagano are with the Department of Computer Science and Systems Engineering, Graduate School of Engineering, Kobe University, 657-8501 Kobe, Japan forestrabo_884@cs11.cs, luo@gold, aknr-ngn@phoenix.kobe-u.ac.jp

K. Kaneko are with the Department of Electrical Engineering, Nagoya University, 464-8601 Nagoya,Japan kaneko.kazuaki@d.mbox.nagoya-u.ac.jp

F. Asano are with the School of Information Science, Japan Advanced Institute of Science and Technology, 923-1292 Nomi,Japan fasano@jaist.ac.jp

A. Kato are with the Department of Electronics, Aichi Institute of Technology, 470-0392 Toyota, Japan katoatuo@aitech.ac.jp

II. EFFECT OF THE COUNTERWEIGHTS

A. Proposed model

We derive the dynamic equation and equation of the inelastic collision to analyze our model. Fig. 1 shows our previous bipedal walking model[3]. Fig. 2 shows the ideal model for the walking machine with counterweights, which has prismatic joints driven by telescopic actuators on each leg. From now on, we call the model shown in Fig. 1 as "Model 1", and the model shown in Fig. 2 as "Model 2". The main physical parameters of Model 2 are identical to Model 1, and in Fig. 2 we highlighted the difference from Fig. 1. In this paper, we introduce counterweights which is the main difference from our previous model [3].

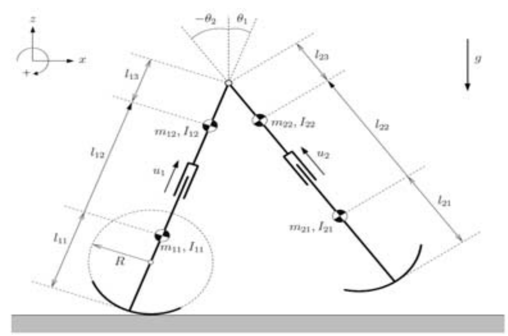

Fig. 1. [Model 1] Simulation model with prismatic joint

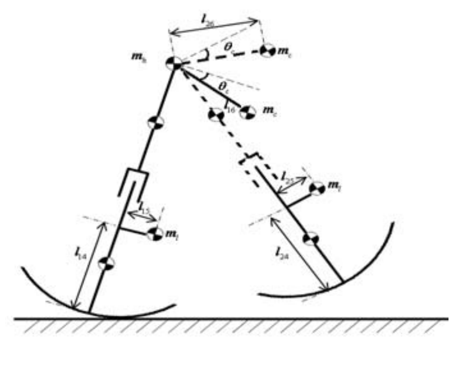

Fig. 2. [Model 2] Simulation model with counterweights and hip mass

B. Dynamic equation of Model 2

Mass, position, angle of the counterweights are described in Fig. 2 as m_c, l_{i6}, and θ_c, respectively. From now on, we call the stance and swing leg "leg1" and "leg2", respectively. We derive the dynamic equation of the legs separately, and connect them at the hip joint by introducing a constraint force. We chose the generalized coordinate vector for the leg i as $\boldsymbol{q}_i = [x_i\ z_i\ \theta_i\ l_{i2}]^{\mathrm{T}}\ (i = 1, 2)$. The dynamic equation of the leg i without any constraint forces is given by

$$\begin{bmatrix} \boldsymbol{M}_1(\boldsymbol{q}_1) & \boldsymbol{0}_{4\times4} \\ \boldsymbol{0}_{4\times4} & \boldsymbol{M}_2(\boldsymbol{q}_2) \end{bmatrix} \begin{bmatrix} \ddot{\boldsymbol{q}}_1 \\ \ddot{\boldsymbol{q}}_2 \end{bmatrix} + \begin{bmatrix} \boldsymbol{h}_1(\boldsymbol{q}_1, \dot{\boldsymbol{q}}_1) \\ \boldsymbol{h}_2(\boldsymbol{q}_2, \dot{\boldsymbol{q}}_2) \end{bmatrix} = \begin{bmatrix} \boldsymbol{S}_1 u_1 \\ \boldsymbol{S}_2 u_2 \end{bmatrix}, \quad (1)$$

where $\boldsymbol{M_i} \in \mathbb{R}^{4\times4}$ is the inertia matrix, $\boldsymbol{h_i} \in \mathbb{R}^4$ is the centrifugal, Coriolis, and gravity vector, and $\boldsymbol{S}_i u_i \in \mathbb{R}^4$ is the control input vector which is given by $\boldsymbol{S}_i u_i = [0\ 0\ 0\ 1]^{\mathrm{T}} u_i\ (i = 1, 2)$, where u_i [N] is the control force of the leg i's telescopic actuator. By taking the constraint forces into account, we can obtain the complete dynamic equation as

$$\begin{bmatrix} \boldsymbol{M}_1(\boldsymbol{q}_1) & \boldsymbol{0}_{4\times4} \\ \boldsymbol{0}_{4\times4} & \boldsymbol{M}_2(\boldsymbol{q}_2) \end{bmatrix} \begin{bmatrix} \ddot{\boldsymbol{q}}_1 \\ \ddot{\boldsymbol{q}}_2 \end{bmatrix} + \begin{bmatrix} \boldsymbol{h}_1(\boldsymbol{q}_1, \dot{\boldsymbol{q}}_1) \\ \boldsymbol{h}_2(\boldsymbol{q}_2, \dot{\boldsymbol{q}}_2) \end{bmatrix} = \begin{bmatrix} \boldsymbol{S}_1 u_1 \\ \boldsymbol{S}_2 u_2 \end{bmatrix} + \boldsymbol{J(q)}^{\mathrm{T}} \boldsymbol{\lambda}, \quad (2)$$

where $\boldsymbol{J(q)}^{\mathrm{T}} \boldsymbol{\lambda} \in \mathbb{R}^8$ indicates the constraint force which comes from the connection of the two legs at the hip joint, also impose the condition on the stance leg which does not slip on the ground. The Jacobian matrix, $\boldsymbol{J}(\boldsymbol{q})$, is determined by using the equation $\boldsymbol{J}(\boldsymbol{q})\dot{\boldsymbol{q}} = \boldsymbol{0}_{4\times1}$. In the following, we simply express the complete dynamic equation as

$$\boldsymbol{M}(\boldsymbol{q})\ddot{\boldsymbol{q}} + \boldsymbol{h}(\boldsymbol{q}, \dot{\boldsymbol{q}}) = \boldsymbol{S}\boldsymbol{u} + \boldsymbol{J}(\boldsymbol{q})^{\mathrm{T}} \boldsymbol{\lambda}, \quad (3)$$

where

$$\boldsymbol{q} := \begin{bmatrix} \boldsymbol{q}_1 \\ \boldsymbol{q}_2 \end{bmatrix}, \ \boldsymbol{S}\boldsymbol{u} := \begin{bmatrix} \boldsymbol{S}_1 & \boldsymbol{0}_{4\times1} \\ \boldsymbol{0}_{4\times1} & \boldsymbol{S}_2 \end{bmatrix} \begin{bmatrix} u_1 \\ u_2 \end{bmatrix}, \quad (4)$$

We now describe velocity constraint conditions for the Jacobian matrix. The velocity constraint conditions are given by differentiating the conditions that two legs' hip positions are identical and the rolling contact conditions between the stance leg and ground. They are expressed as

$$\begin{aligned} &\dot{x_1} + \dot{l_{12}} \sin\theta_1 + (l_{13} + l_{12}) \cos\theta_1 \dot{\theta_1} \\ &= \dot{x_2} + \dot{l_{22}} \sin\theta_2 + (l_{23} + l_{22}) \cos\theta_2 \dot{\theta_2}, \end{aligned} \quad (5)$$

$$\begin{aligned} &\dot{z_1} + \dot{l_{12}} \cos\theta_1 - (l_{13} + l_{12}) \sin\theta_1 \dot{\theta_1} \\ &= \dot{z_2} + \dot{l_{22}} \cos\theta_2 - (l_{23} + l_{22}) \sin\theta_2 \dot{\theta_2}, \end{aligned} \quad (6)$$

$$\dot{x_1} = R\dot{\theta_1}, \ \dot{z_1} = 0, \quad (7)$$

The Jacobian matrix is derived by putting the four velocity constraint conditions into equation $\boldsymbol{J}(\boldsymbol{q})\dot{\boldsymbol{q}} = \boldsymbol{0}_{4\times1}$.

C. Equation of inelastic collision for heel-strike

The equation of inelastic collision with the ground can be expressed as

$$\boldsymbol{M}(\boldsymbol{q})\dot{\boldsymbol{q}}^+ = \boldsymbol{M}(\boldsymbol{q})\dot{\boldsymbol{q}}^- + \boldsymbol{J_I}(\boldsymbol{q})^{\mathrm{T}} \boldsymbol{\lambda_I}, \quad (8)$$

where $\boldsymbol{J_I}^{\mathrm{T}} \boldsymbol{\lambda_I} \in \mathbb{R}^8$ denotes the constraint force at heel-strike and the Jacobian matrix at heel-strike, $\boldsymbol{J_I}$, should satisfy the following equation:

$$\boldsymbol{J}_I(\boldsymbol{q})\dot{\boldsymbol{q}}^+ = \boldsymbol{0}_{6\times1}, \quad (9)$$

The superscripts "−" and "+" indicate just-before and just-after the impact, respectively. Using Eqs. (8) and (9), we can get the relation between $\dot{\boldsymbol{q}}^+$ and $\dot{\boldsymbol{q}}^-$. It is expressed as

$$\dot{\boldsymbol{q}}^+ = (\boldsymbol{I}_8 - \boldsymbol{M}^{-1} \boldsymbol{J}_I^{\mathrm{T}} \boldsymbol{X_I}^{-1} \boldsymbol{J}_I)\dot{\boldsymbol{q}}^-, \quad (10)$$

where $\boldsymbol{X_I} := \boldsymbol{J_I} \boldsymbol{M}^{-1} \boldsymbol{J_I}^{\mathrm{T}}$. To get the detailed Jacobian matrix at heel-strike, we need to derive the velocity constraint condition. In this situation, our model should satisfy Eqs. (5) and (6), and we also have to consider the following conditions of leg 2 that expresses the rolling contact with the ground:

$$\dot{x_2}^+ = R\dot{\theta_2}^+, \ \dot{z_2}^+ = 0, \quad (11)$$

In addition, the constraint conditions for mechanical lock of the telescopic joints are expressed as

$$\dot{l_{12}}^+ = 0, \ \dot{l_{22}}^+ = 0, \quad (12)$$

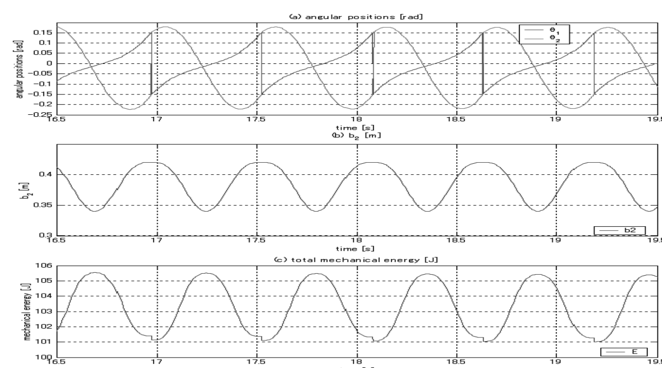

Fig. 3. Simulation results of Model 2

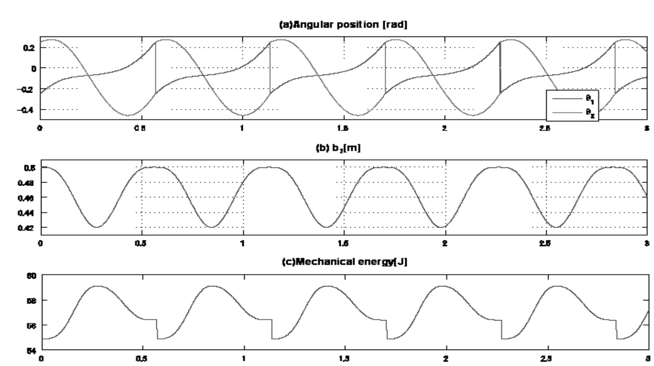

Fig. 4. Simulation results of Model 1

The Jacobian matrix, $\boldsymbol{J}_I(\boldsymbol{q})$, is then given by summarizing the six velocity constraint conditions of Eqs. (5), (6), (7), and (11).

D. Control law

We chose the following desired-time trajectory of l_{22} as follows

$$l_{22d}(t) = \begin{cases} l_{22max} - A\sin^3(\frac{\pi}{T_{set}}t) & (0 \le t \le T_{set}) \\ l_{22max} & (t \ge T_{set}) \end{cases}, \quad (13)$$

Our purpose is making the length of telescopic joints follow the above equation's l_{22d} by giving the controlling input in the actuator. The length of telescopic joints is expressed as $\boldsymbol{l_2} = [l_{12}\ \ l_{22}]^{\mathrm{T}}$. This vector is expressed using the generalized coordinates as $\boldsymbol{l_2} = \boldsymbol{S}^{\mathrm{T}}\boldsymbol{q}$,its second order derivative with respect to time yields

$$\ddot{\boldsymbol{l_2}} = \boldsymbol{S}^{\mathrm{T}}\ddot{\boldsymbol{q}} = \boldsymbol{S}^{\mathrm{T}}(\boldsymbol{M}^{-1}(\boldsymbol{Su}-\boldsymbol{h}) + \boldsymbol{M}^{-1}\boldsymbol{J}^{\mathrm{T}}\boldsymbol{\lambda}), \quad (14)$$

We can solve the Eqs. (14) for $\boldsymbol{\lambda}$ with following the equation $\boldsymbol{J}\ddot{\boldsymbol{q}} = -\dot{\boldsymbol{J}}\dot{\boldsymbol{q}}$. $\boldsymbol{\lambda}$ is expressed as

$$\boldsymbol{\lambda} = \boldsymbol{X}^{-1}(-\dot{\boldsymbol{J}}\dot{\boldsymbol{q}} - \boldsymbol{J}\boldsymbol{M}^{-1}(\boldsymbol{Su}-\boldsymbol{h})), \quad (15)$$

where $\boldsymbol{X} = \boldsymbol{J}\boldsymbol{M}^{-1}\boldsymbol{J}^{\mathrm{T}}$. By substituting this into Eq. (14), we can obtain the following equation.

$$\ddot{\boldsymbol{l_2}} = \boldsymbol{Fu} + \boldsymbol{G} \quad (16)$$

where

$$\begin{aligned} \boldsymbol{F} &:= \boldsymbol{S}^{\mathrm{T}}\boldsymbol{M}^{-1}(\boldsymbol{M} - \boldsymbol{J}^{\mathrm{T}}\boldsymbol{X}^{-1}\boldsymbol{J})\boldsymbol{M}^{-1}\boldsymbol{S}, \quad (17)\\ \boldsymbol{G} &:= -\boldsymbol{S}^{\mathrm{T}}\boldsymbol{M}^{-1}\boldsymbol{h} - \boldsymbol{S}^{\mathrm{T}}\boldsymbol{M}^{-1}\boldsymbol{J}^{\mathrm{T}}\boldsymbol{X}^{-1}\dot{\boldsymbol{J}}\dot{\boldsymbol{q}} \\ &\quad + \boldsymbol{S}^{\mathrm{T}}\boldsymbol{M}^{-1}\boldsymbol{J}^{\mathrm{T}}\boldsymbol{X}^{-1}\boldsymbol{J}\boldsymbol{M}^{-1}\boldsymbol{h}, \quad (18) \end{aligned}$$

Then we chose the controlling input follow as

$$\begin{aligned} \boldsymbol{u} &= \boldsymbol{F}^{-1}(\bar{\boldsymbol{u}} - \boldsymbol{G}), \quad (19)\\ \bar{\boldsymbol{u}} &= \ddot{\boldsymbol{l_{2d}}} + \boldsymbol{K}_D(\dot{\boldsymbol{l_{2d}}} - \dot{\boldsymbol{l_2}}) + \boldsymbol{K}_P(\boldsymbol{l_{2d}} - \boldsymbol{l_2}), \quad (20) \end{aligned}$$

where $\boldsymbol{l_{2d}} = [l_{12d}\ \ l_{22d}]^{\mathrm{T}}$, $\boldsymbol{K}_D \in \mathbb{R}^{2\times 2}$ and $\boldsymbol{K}_P \in \mathbb{R}^{2\times 2}$ are PD gain matrices.

E. Simulation studies

1) Difference between Model 1 and Model 2: We chose the m_c, l_{i6} improving the gait best at this angle with physical parameter shown in TABLE I. Fig. 3 and Fig. 4 shows the simulation results of each model ; leg angles, l_{22} and the mechanical energy. We can see both Fig 3 and 4 have the same tendency and having a stable step. The difference between the two results is (C) Mechanical energy. Both models need about 5[J] to pumping the leg to recover the mechanical energy, lost by the heel strike. When investigating the lost energy, Mode 2 loses one fourth less then Model 2. This means Model 2 is having a smoother step.

TABLE I

PHYSICAL PARAMETER USED FOR EXPERIMENTATION

l_{i1}	0.56	m	m_{i1}	5.60	kg
l_{i2max}	0.42	m	m_{i2}	1.55	kg
l_{i3}	0.10	m	m_l	0	kg
l_{i4}	0.30	m	m_H	0.56	kg
l_{i5}	0.03	m	m_c	0.05	kg
l_{i6}	0.17	m	A	0.08	m
R	0.50	m	T_{set}	0.55	s
			θ_c	1.18	rad

TABLE II

EFFECTS OF COUNTERWEIGHTS WHERE $A = 0.08$ [M]

	Model 1	model 2
Walking speed [m/s]	0.5523	0.6100
Restored mechanical energy [J]	0.2076	0.2960
Specific resistance [-]	0.1921	0.1723

TABLE III

EFFECTS OF COUNTERWEIGHTS WHERE $A = 0.10$ [M]

	Model 1	Model 2
Walking speed [m/s]	0.5523	0.9358
Restored mechanical energy [J]	0.2076	2.9977
Specific resistance [-]	0.1921	0.1260

2) Counterweights effect: Here, we analyze the effect of the counterweights in our model through computer simulation by MATLAB. In detail, to evaluate the effects of the counterweights we changed the parameter m_c, l_{i6}, θ_c regarding to the counterweights, and observed next 3 results walking speed, restore of the mechanical energy in one step and specific resistance. Figs. 5 to 8 show the effects of changing the length of counterweights at each m_c. We chose θ_c as $-0.52, 0.0, 0.79, 1.18$ [rad] to get the rough trend. Figs. 5 and 6 ($\theta_c = -0.52, 0.0$ [rad]) indicate that extending the length of counterweights decrease the walking speed and restored mechanical energy in one step in this angle range. On the other hand, values of specific resistance increase with extension of the counterweights. It means that the extension of the counterweights make the machine's efficiency worse. Fig. 7 ($\theta_c = 0.79$ [rad]) shows that the extension of counterweights makes the walking speed and the restored mechanical energy in one step greater. Furthermore, the specific resistance is improved by the extension at this angle. Fig. 8 shows that $\theta_c = 1.18$ [rad] is the best angle to give the machine excellent effects compared with the machine having no counterweights as shown in TABLE II. It shows significant improvement of walking speed, restored mechanical energy, specific resistance. The counterweights'position at $\theta_c = -0.52, 0.0$ [rad] is higher than that of at $\theta_c = 0.79, 1.18$ [rad]. It means that the former position has larger potential energy than the latter. Large potential energy of the counterweights disturbs the excitation of mechanical energy of leg2. For the same reason, our machine is not able to realize stable gait with too heavy counterweights. We conducted the same evaluation of the counterweights at $A = 0.10$ [m] (amplitude of telescopic joints). This change brought out the great ability of the counterweights. This time significant effects by counterweights also appears at $\theta_c = 1.18$ [rad]. Detailed effects is shown in TABLE III.This improvement comes from the fact that increased mechanical energy resist the heavy counterweights. If counterweights are

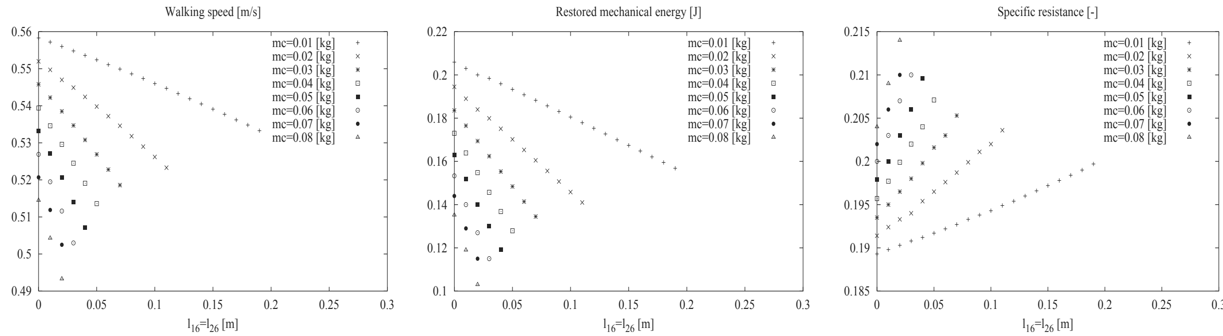

Fig. 5. Gait descriptors with respect to l_{i6} [m] for eight values of m_c [kg] where $T_{set} = 0.55$ [s], $A = 0.08$ [m], $\theta_c = -0.52$ [rad]

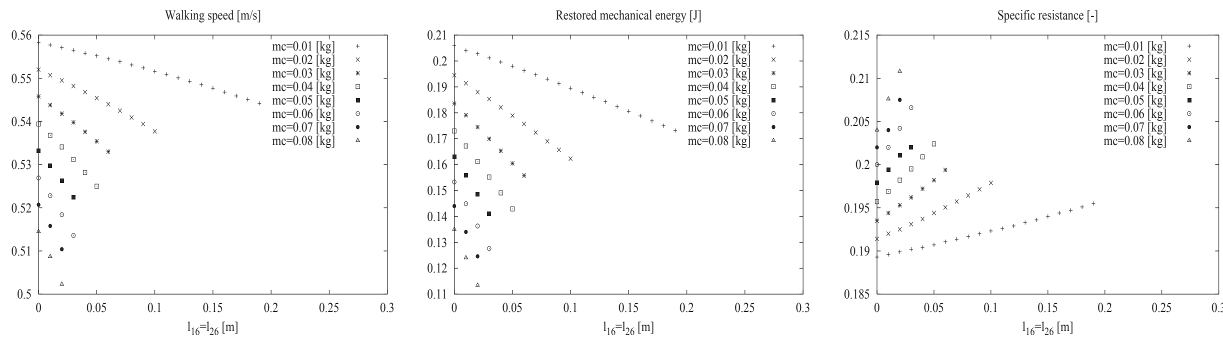

Fig. 6. Gait descriptors with respect to l_{i6} [m] for eight values of m_c [kg] where $T_{set} = 0.55$ [s], $A = 0.08$ [m], $\theta_c = 0.0$ [rad]

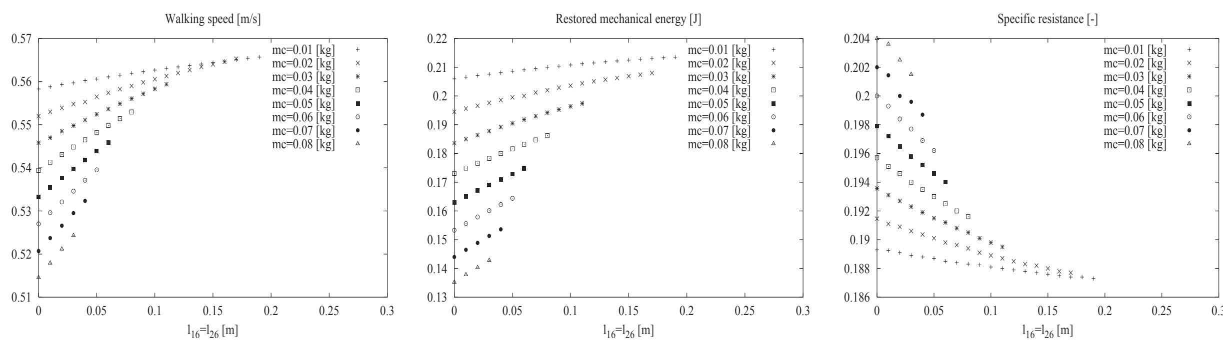

Fig. 7. Gait descriptors with respect to l_{i6} [m] for eight values of m_c [kg] where $T_{set} = 0.55$ [s], $A = 0.08$ [m], $\theta_c = 0.79$ [rad]

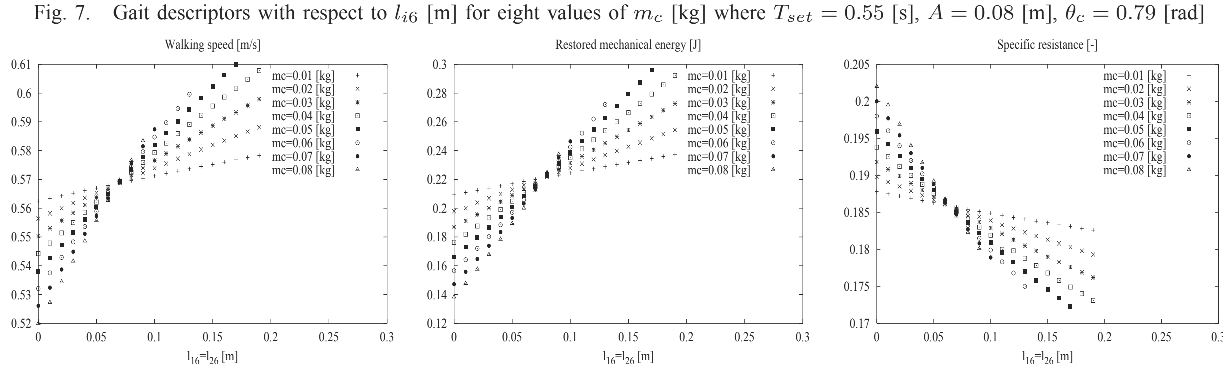

Fig. 8. Gait descriptors with respect to l_{i6} [m] for eight values of m_c [kg] where $T_{set} = 0.55$ [s], $A = 0.08$ [m], $\theta_c = 1.18$ [rad]

attached on appropriate position,the machine is given greater drive than that of previous condition.

III. DEVELOPMENT OF THE WALKING MACHINE

We have developed a waking machine which has telescopic legs, semicircular feet, free hip-joint, and counterweights as shown in Fig. 9 and 10. In this section we will describe the detail of our walking machine.

A. Walker's mechanism

The experimental devices that we used are on recoded [3], also Table IV gives the physical parameters of the biped robot. The values for the items named "arbitrary" can be chosen from free wide range, the values in parentheses have a mechanical limit. This comes from our previous work [3], that mass ratio comprises an important part on

TABLE IV

PHYSICAL PARAMETER SETTINGS FOR EXPERIMENTAL MACHINE

l_{l1}	0.5 m	m_2	1.6 (+0 – 0.5) kg
l_{l2}	0.3 (+0 – 0.12) m	m_l	0 (+0 – 3.5) kg
l_{l3}	0.2 m	m_c	voluntarily mass kg
x_{li}, y_{li}	arbitrary length m	m_h	0(+0 – 2.2) kg
x_{hi}, y_{hi}	arbitrary length m	θ_{H1}	arbitrary angle rad
R	0.5 m	θ_{H2}	arbitrary angle rad
m_1	5.6 kg		

the control performances. One of the characteristic points of our machine is that each leg has an attachment for the counterweights which is identical to the simulation model in the previous section. Also binding the two legs, both inside and the outside, physically limits the motion into two dimensions.

B. Control system

We chose C-CHIP as the main-computer for the purpose of developing the robot autonomous. C-CHIP is a very small controller which was designed at AIT and BMC, RIKEN. It is constituted by several modules and the machine ability depends on how it is combined. The detail of the modules which we used is described in our previous work[3]. By using this C-CHIP, we succeeded in moving four legs perfectly without wires.

Fig. 11 is the overview of our systems. The difference between the system and our previous report [3] is that here we added the walking cycle resetting system to feedback the data to the main computer. Before using this cycle resetting system, it was very rare to walk successfully. This is because it is very difficult to swithch the two cycles seamlessly; prismatic joint pumping cycle and the walking period cycle. To solve this problem we use the microswitch to obtain the timing of the heel strike, and by using those strike date, we made the desired time-trajectory of the leg signal to follow the initial condition.

IV. EXPERIMENTAL RESULTS

By using the robot shown in Fig. 9 sustainable level dynamic walking had been achieved only up to 5 steps. The reason for this low success is that we could not give the same initial condition. We can see from Fig. 4 that at this model the impact of the heel strike is very large, and so the initial condition becomes a very critical factor. On the other hand from Fig. 3, the importance of the heel strike impact is lesser. Fig. 12 shows the experimental result using Fig. 10. By using the counterweights attached model, the success probability of the walking experiment increased. The experimental results when changing the length of the counterweights are shown in Fig. 13 and 14. Also from Fig. 13 we can see a tendency similar to Fig. 8;increasing the counterweight length and mass, the walking speed gets faster. Using Fig.10 we had observation of more than 8 steps with the probability of one fourth in the experiment. In addition, we had a record of 4[m] walks; witch was the limit of the experimental environment.

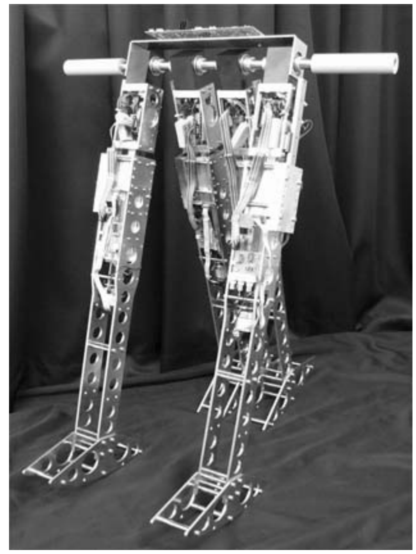

Fig. 9. Overview of Model 1 parametric excitation biped robot

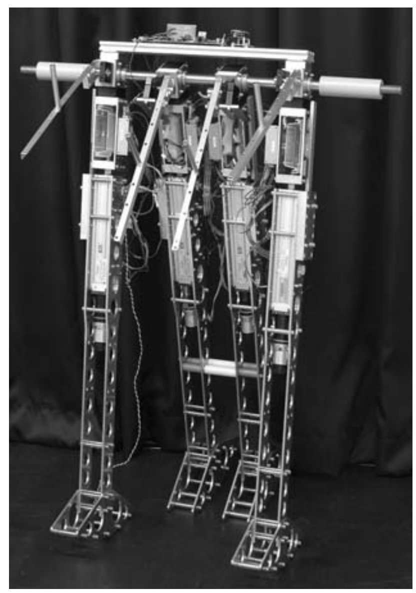

Fig. 10. Overview of Model 2 parametric excitation biped robot with counterweights

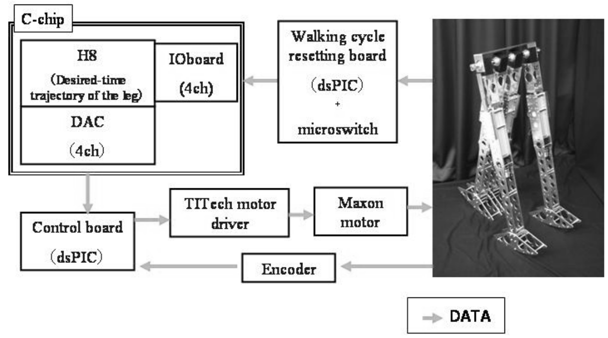

Fig. 11. Experimental apparatus

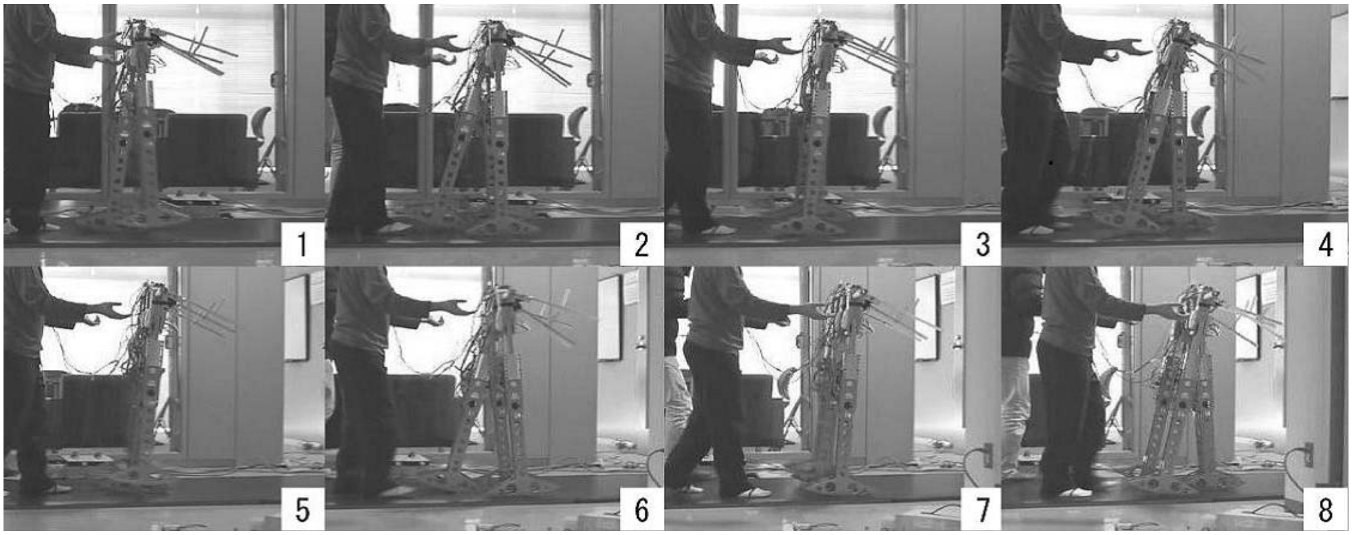

Fig. 12. Snapshots of successful parametrically excited dynamic bipedal walking

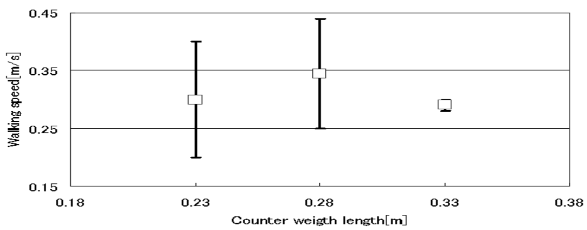

Fig. 13. Average walking speed

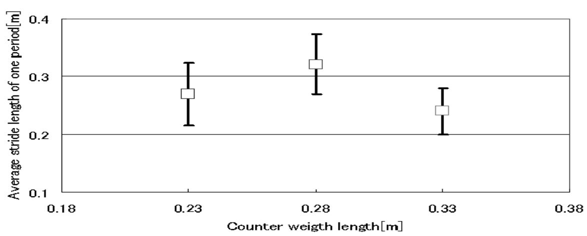

Fig. 14. Average stride length of one period

V. CONCLUSION AND FUTURE WORK

In this paper, we studied the effect of the counterweights for parametrically excited dynamic bipedal walking. Through numerical simulation we showed that when the counter-weights attached on the appropriate position, the robot can walk faster and more efficiently. In the experiment, we could finally generate a sustainable level dynamic gait by the effect of the counterweights.

Now we are studying another approach to parametrically excited walking based on knee-joint actuation [9] and [10]. Parametric excitation is also possible in even general kneed walkers without prismatic joints, and the results will be reported in another paper.

Future work in our experiment is to evaluate the effectiveness of the counterweights based on experimental data. Traversing rugged terrain, improvement of energy-efficiency using elastic elements, and achieving stable walking by stance-leg actuation [10] are also left as the future work.

VI. ACKNOWLEDGMENTS

This work was partially supported by a Grant-in-Aid for Scientific Research, (B) No. 18360115, provided by the Japan Society for the Promotion of Science (JSPS). The authors would like to acknowledge the assistance, support, and efforts of S. Hirano, Y. Harata and laboratory members of AIT; Mr.T. Ito, and Mr. K.Kurachi.

REFERENCES

[1] S. Collins, A. Ruina, R. Tedrake, and M. Wisse, "Efficient bipedal robots based on passive dynamic walkers," *Science Magazine*, Vol. 307, No. 5712, pp. 1082–1085, 2005.

[2] T. McGeer, "Passive dynamic walking," *Int. J. of Robotics Research*, Vol. 9, No. 2, pp. 62–82, 1990.

[3] F. Asano, T. Hayashi, S. Hirano, Z.W. Luo, and A. Kato, "Parametric excitation approaches to efficient dynamic bipedal walking," *Proc. of the IEEE/RSJ Int. Conf. on Intelligent Robots and Systems*, 2007.

[4] F. Asano, M. Yamakita, N. Kamamichi, and Z.W. Luo, "A novel gait generation for biped walking robots based on mechanical energy constraint," *IEEE Trans. on Robotics and Automation*, Vol. 20, No. 3, pp. 565–573, 2004.

[5] F. Asano, Z.W. Luo, and M. Yamakita, "Biped gait generation and control based on a unified property of passive dynamic walking," *IEEE Trans. on Robotics*, Vol. 21, No. 4, pp. 754–762, 2005.

[6] F. Asano and Z.W. Luo, "On energy-efficient and high-speed dynamic biped locomotion with semicircular feet," *Proc. of the IEEE/RSJ Int. Conf. on Intelligent Robots and Systems*, pp. 5901–5906, 2006.

[7] F. Asano and Z.W. Luo, "Dynamic analyses of underactuated virtual passive dynamic walking," *Proc. of the IEEE Int. Conf. on Robotics and Automation*, pp. 3210–3217, 2007.

[8] F. Asano and Z.W. Luo, "The effect of semicircular feet on energy dissipation by heel-strike in dynamic biped locomotion," *Proc. of the IEEE Int. Conf. on Robotics and Automation*, pp. 3976–3981, 2007.

[9] Y. Harata, F. Asano, Z.W. Luo, K. Taji, and Y. Uno, "Biped gait generation based on parametric excitation by knee-joint actuation," *Proc. of the IEEE/RSJ Int. Conf. on Intelligent Robots and Systems*, pp. 2198–2203, 2007.

[10] T.Honjo, A.Nagano and Z.W.Luo, "Parametric Excitation of a Biped Robot as an Inverted Pendulum," *Proc. of the IEEE/RSJ Int. Conf. on Intelligent Robots and Systems*, 2008.